archives
of thermodynamics
Vol. **35**(2014), No. 2, 3–20
DOI: 10.2478/aoter-2014-0010

Pool boiling of nanofluids on rough and porous coated tubes: experimental and correlation

JANUSZ T. CIEŚLIŃSKI*
TOMASZ Z. KACZMARCZYK

Gdańsk University of Technology, Faculty of Mechanical Engineering, Narutowicza 11/12, 80-233 Gdańsk, Poland

Abstract The paper deals with pool boiling of water-Al_2O_3 and water-Cu nanofluids on rough and porous coated horizontal tubes. Commercially available stainless steel tubes having 10 mm outside diameter and 0.6 mm wall thickness were used to fabricate the test heater. The tube surface was roughed with emery paper 360 or polished with abrasive compound. Aluminium porous coatings of 0.15 mm thick with porosity of about 40% were produced by plasma spraying. The experiments were conducted under different absolute operating pressures, i.e., 200, 100, and 10 kPa. Nanoparticles were tested at the concentration of 0.01, 0.1, and 1% by weight. Ultrasonic vibration was used in order to stabilize the dispersion of the nanoparticles. It was observed that independent of operating pressure and roughness of the stainless steel tubes addition of even small amount of nanoparticles augments heat transfer in comparison to boiling of distilled water. Contrary to rough tubes boiling heat transfer coefficient of tested nanofluids on porous coated tubes was lower compared to that for distilled water while boiling on porous coated tubes. A correlation equation for prediction of the average heat transfer coefficient during boiling of nanofluids on smooth, rough and porous coated tubes is proposed. The correlation includes all tested variables in dimensionless form and is valid for low heat flux, i.e., below 100 kW/m^2.

Keywords: Pool boiling; Nanofluids; Correlation equation; Rough and porous coated tubes

*Corresponding Author. E-mail: jcieslin@pg.gda.pl

Nomenclature

C_{sf}	–	liquid-surface parameter
a	–	average pore radius, μm
c_p	–	specific heat at constant pressure, J/(kgK)
D	–	diameter, m
g	–	acceleration due to gravity, m/s^2
I	–	current, A
K	–	surface state parameter
L	–	length, m
P	–	electrical power, W
p	–	pressure, Pa
q	–	heat flux, W/m^2
r	–	latent heat of vaporization, J/kg
R_a	–	mean surface roughness, μm
R_z	–	maximum roughness depth, μm
R_q	–	root mean square roughness, μm
T	–	temperature, °C
U	–	voltage, V

Greek symbols

α	–	mean heat transfer coefficient, W/(m^{2}K)
Φ	–	nanoparticle concentration, %
λ	–	thermal conductivity, W/(mK)
ρ	–	density, kg/m^3
σ	–	surface tension, N/m^2
μ	–	viscosity, Pa s

Subscripts

cor	–	correlation
cr	–	critical
exp	–	experimental
f	–	fluid
i	–	inside
l	–	liquid
loc	–	local
o	–	outside
p	–	particle
t	–	tube
v	–	vapour
w	–	wall

Dimensionless numbers

$\nu = \dfrac{\alpha D_o}{\lambda_l}$	–	Nusselt number
$\mathrm{Bo} = \dfrac{qL\rho_l}{\rho_v r \mu_l}$	–	boiling number
$L = \sqrt{\dfrac{\sigma}{g(\rho_l - \rho_v)}})$	–	characteristic length

1 Introduction

Boiling heat transfer rate depends on coupling of heating surface state and working fluid properties. Augmentation of heat transfer during boiling was based so far mostly on modification of the surface state. Little attention was paid to alteration of thermophysical properties of boiling liquid. In 1995 a group in Argonne National Laboratory, USA, has developed a new category of fluids termed nanofluids [1]. Nanofluid is a suspension consisting of the base liquid and metallic or non-metallic nanoparticles with sizes significantly smaller than 100 nm. Due to distinct augmentation of thermal conductivity in comparison with base liquid, nanofluids could provide a basis for an innovation for heat transfer intensification. Regarding boiling heat transfer some studies report no change of heat transfer, some report heat transfer deterioration and others the heat transfer enhancement [2]. Significant critical heat flux (CHF) enhancement occurs with various nanoparticle materials at relatively low concentrations [3]. The boiling heat transfer can be intensified by increasing the number of active centres of vapour generation and also by increasing the heat supply to vapour bubbles in the process of their growth. This can be obtained by creating different surface conditions such as micro- and macroroughness, finning, vibrorolling, tunnel-and-pore-forming, and porous coatings [4–6]. Many aspects of pool boiling of nanofluids were investigated, among others effect of concentration of nanoparticles, effect of nanoparticle material, effect of heating surface orientation, material and finish, effect of base liquid, and effect of operating pressure [7,8].

Relatively small number of publications are devoted to the pool boiling of nanofluids on rough surfaces. Das *et al.* [9,10] observed that the nanoparticles degrade the boiling performance systematically with increasing Al_2O_3 particle concentration (1, 2 and 4% by volume) resulting in an increase of wall superheat for a given heat flux. The deterioration in boiling performance is observed to be more drastic at higher surface roughness (R_a = 0.4 and 1.15 μm). Khandekar *et al.* [11] established that the surface roughness of the sample after boiling of water-Al_2O_3, water-CuO and water-laponite clay nanofluids with 1% concentration by weight, was lower than the original substrate. The initial surface roughness of the substrate was found to be $R_a = 0.23$ μm, $R_z = 1.78$ μm, and $R_q = 0.29$ μm. After two hours of boiling the surface roughness was found to be $R_a = 0.20$ μm, $R_z = 1.66$ μm, and $R_q = 0.25$ μm for the case of alumina and $R_a = 0.18$ μm, $R_z = 1.62$ μm, and $R_q = 0.24$ μm for laponite clay based nanofluid. Ac-

cording to Khandekar *et al.* [11] the nanoparticles are getting entrapped in the nucleating surface cavities thereby reducing their size and degrading the active nucleation density. Chopkar *et al.* [12] confirmed Das *et al.* [9,10] results, that with the repetition of experiment with water-ZrO_2 nanofluids on flat copper plate, both surface roughness and the boiling heat transfer coefficient decreased. Suriyawong and Wongwises [13] carried out a systematic study of heat transfer during boiling of water-TiO_2 nanofluids with volume concentrations of 0.00005, 0.0001, 0.0005, 0.005, and 0.01% on copper and aluminium substrate surfaces. The heating surfaces had average roughness of 0.2 and 4 μm. Suriyawong and Wongwises [13] found that for nanofluid with nanoparticle concentration of 0.00001% while boiling on a copper surface the heat transfer coefficient increased by an average of 15% with a surface roughness of 0.2 μm and at 4% with a surface roughness of 4 μm. Moreover, it was established that with the same heating surface material the roughness of 4 μm gave a higher heat transfer coefficient than the roughness of 0.2 μm by about 12%. Narayan *et al.* [14] suggested, that final effect of enhancement or deterioration of heat transfer during boiling on rough surfaces depends on the ratio of mean roughness to the nanoparticle diameter R_a/D_p. They found a maximum deterioration at $R_a/D_p = 1$. The pool boiling heat transfer coefficient was enhanced when the nanoparticles were either much larger or much smaller than the size of the heater surface roughness.

Only a few publications are devoted to the pool boiling of nanofluids on enhanced surfaces. Liu *et al.* [15] studied pool boiling of water-CuO nanofluid of several nanoparticle concentrations from 0.1% to 2% by weight on horizontal copper plate with microgrooves. The experiments were conducted under four operating pressures of 7.4, 20, 31.2, and 100 kPa. Independent of operating pressure significant heat transfer enhancement was observed for nanoparticle concentrations lower than 1%. For nanoparticle concentrations above 1% heat transfer deterioration was recorded. For optimum nanoparticle concentration of 1% and operating pressure of 7.4 kPa heat transfer coefficient for nanofluid was about two times higher than for pure water. Yang and Liu [16] carried out experiments with boiling of R141b-Au nanofluids on horizontal structured and porous coated tubes with outside diameter ranging from 18 to 19.5 mm. The concentration of nanoparticles was 0.09 and 0.4% respectively by volume. For structured tube, with so called re-entrant cavities, results obtained for refrigerant R141b-Au nanofluids – independent of nanoparticle concentration, overlap with that for a pure re-

frigerant. For porous coated tube and heat flux below 35 kW/m^2, higher heat transfer coefficient was obtained for pure refrigerant – independent of nanoparticle concentration. For heat flux above 35 kW/m^2 and lower nanoparticle concentration, i.e., 0.09%, higher heat transfer coefficient was obtained for R141b-Au nanofluid.

It seems that Das *et al.* [17] were the first that proposed Cornwell-Houston [18] type correlations for pool boiling of water-Al_2O_3 nanofluids separately for smooth and rough tubes and each nanoparticle concentration. Shi *et al.* [19] developed a Nusselt type correlation for pool boiling of water-Fe nanofluids with nanoparticle concentration of 2 vol%. Building on Rohsenow correlation [20], Das and Bhaumik [21] proposed a correlation for heat flux prediction during pool boiling of water-Al_2O_3 and water-TiO_2 nanofluids at different nanoparticle concentrations with respect to the temperature in mechanically polished flat stainless steel plate. Using Stephan and Abdelsalam correlation [22], Peng *et al.* [23] elaborated the nucleate pool boiling heat transfer correlation for refrigerant-based nanofluid with surfactant. The correlation includes, among others, nanoparticle as well as surfactant concentrations. Pal and Bhaumik [24] developed Rohsenow type correlation [20] for water-TiO_2 nanofluids boiling on stainless steel plate. Knowing different thermal properties of nanofluid and heating surface properties the correlation may be used for prediction of heat flux and subsequently boiling heat transfer coefficient. Suriyawong *et al.* [25] elaborated correlation for predicting heat transfer coefficient for nucleate pool boiling of water-TiO_2 nanofluids on horizontal circular plates made from copper and aluminium at low concentrations. The proposed correlation consists of various relevant factors, besides the thermal properties of the nanofluid, the roughness of heating surface and the volume fraction of nanoparticles.

The main aim of the present study was to obtain boiling characteristics, i.e., boiling curves and heat transfer coefficients for water-Al_2O_3 and water-Cu nanofluids while boiling on horizontal, rough and porous coated tubes under different absolute operating pressure, i.e., 200 kPa, 100 kPa and 10 kPa for three nanoparticle concentrations, i.e. of 0.01%, 0.1%, and 1% by weight. Additionally, an approach to develop a correlation equation for prediction of average heat transfer coefficient during boiling of nanofluids on smooth, rough and porous coated tubes has been undertaken.

2 Experimental setup

2.1 Experimental apparatus

Figure 1 shows a schematic diagram of the experimental apparatus. The test chamber consisted of a cubical vessel made of stainless steel with inside dimensions of 150 mm × 150 mm × 250 mm. Experiments were performed for three values of absolute pressure in the test chamber, i.e., 200, 100, and 10 kPa.

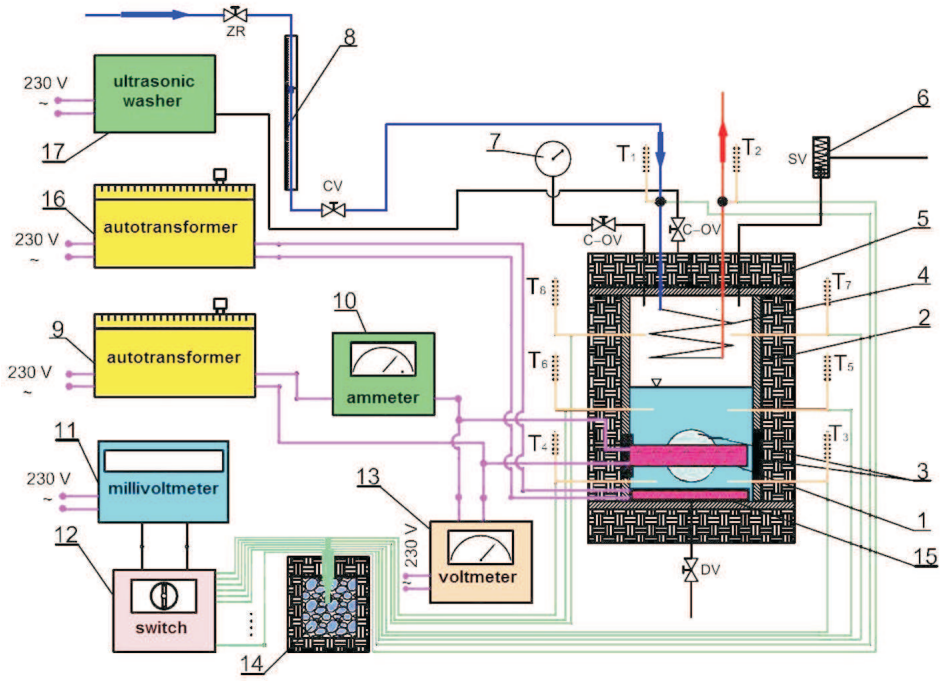

Figure 1: Scheme of the experimental rig: 1 – heating section, 2 – experimental vessel, 3 – inspection windows, 4 – condenser, 5 – insulation, 6 – safety-valve, 7 – manometer, 8 – rotameter, 9 – autotransformer, 10 – ammeter, 11 – millivoltmeter, 12 – switch, 13 – voltmeter, 14 – ice-point, 15 – auxiliary heater, 16 – autotransformer, 17 – ultrasonic washer, T_1, T_2, ... T_7 – thermoelements, DV – drain valve, CV – control valve, C-OV – cut-off valve, SV – safety-valve.

2.2 Heating section

Commercially available stainless steel tubes having outside diameter of 10 mm and 0.6 mm wall thickness were used to fabricate the test heater. The effective length of a tube was 100 mm. A resistance cartridge heater was inserted into the test tube to generate heat flux from an electrical power supply. The power supply can be adjusted by an electrical transformer. Great care must be exercised with the cartridge heater and temperature measuring instrumentation to ensure good accuracy of the measurement of the inside temperature of the heating cylinder. The final design of present heating section has been established after many practical trials supported by numerical simulations of 3D temperature fields. Twelve K-type thermocouples installed in the grooves of a copper sleeve placed inside the tube were used to measure inside temperature of the tube. The detailed geometry of the test tube is shown in Fig. 2. The tube surface was roughed with emery paper 360 or polished with abrasive compound, so the surface roughness was estimated as $R_a = 0.11$ and 0.06 μm, respectively. Aluminium 0.15 mm thick porous coatings with porosity of about 40% were produced by plasma spraying. The pore size distribution was determined by metallographic scanning. For that purpose Super Vist and Svistmet systems were used. A sufficient number of image fields were analyzed so that a statistically reliable result was obtained. The mean pore radius was estimated as equal to 2.8 μm. Figure 3 shows the image of the metallographic specimen of the metallic porous coating.

2.3 Preparation and characterization of the tested nanofluids

In this study Al_2O_3 and copper nanoparticles were used while distilled, deionized water was applied as a base fluid. Nanofluids with different concentrations were prepared for the experiments. Nanoparticles of the required amount and base liquid were mixed together. Ultrasonic vibration was used for 4 h in order to stabilise the dispersion of the nanoparticles. Alumina (Al_2O_3) and copper nanoparticles were tested at the concentration of 0.01, 0.1, and 1% by weight. Alumina nanoparticles, of spherical form have a diameter ranging from 5 to 250 nm; their mean diameter was estimated to be 47 nm according to the manufacturer (Sigma-Aldrich Co.). Copper nanoparticles, of spherical form, have a diameter ranging from 7 to 257 nm; their mean diameter was estimated to be 48 nm according to the manu-

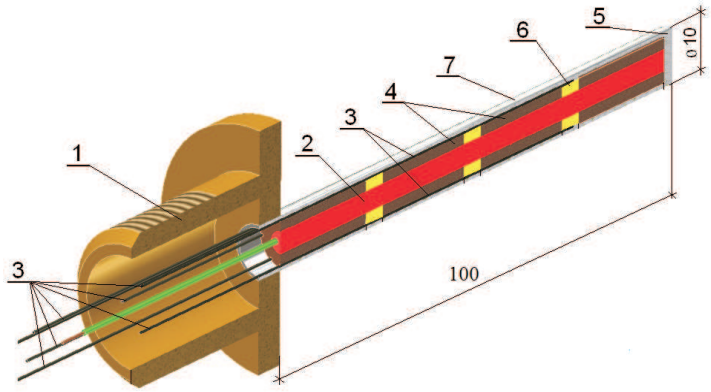

Figure 2: Details of the test section: 1 – flange, 2 – cartridge heater, 3 – thermocouples type K, 4 – copper sleeve, 5 – insulating cap, 6 – Teflon ring, 7 – heating surface.

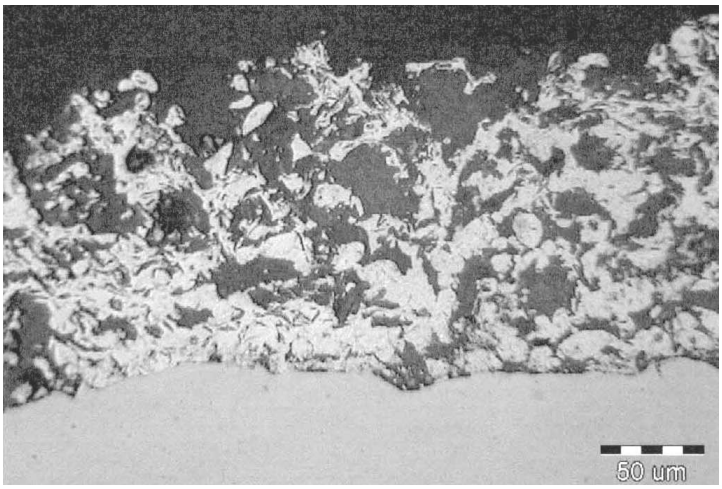

Figure 3: Image of the metallographic specimen of the porous coating.

facturer. The measured pH values for Al_2O_3 nanofluids with nanoparticle concentration of 0.01%, 0.1% and 1% were 6.51, 7.48, and 8.11, respectively. The measured pH values for Cu nanofluids with nanoparticle concentration of 0.01, 0.1 and 1% were 7.44, 6.30, and 6.87, respectively. The stability of the produced nanofluids was pretty good, which means they could stay for a few days without visually observable sedimentation.

2.4 Experimental procedure

The liquid level was maintained at about 15 mm above the centreline of the test tube. In a typical experiment, before the test begins, a vacuum pump was used to evacuate the accumulated air from the vessel. Nanofluid at a preset concentration was charged and then preheated to the saturated temperature by the auxiliary heater. Next, the cartridge heater was switched on. Measurements were first performed at the lowest power input. Data were collected by increasing the heat flux by small increments. In order to ensure consistent surface state after each test the boiling surface was prepared in the same manner, i.e., the stainless steel tube was roughed with emery paper 360 or polished with abrasive compound and next the test tube was placed in an ultrasonic cleaner for 1 h. Finally, the boiling surface was cleaned by water jet.

2.5 Data reduction and uncertainty estimation

Heat flux was calculated as

$$q = \frac{UI}{\pi D_o L_t} = \frac{P}{\pi D_o L_t} \,. \tag{1}$$

The wall temperature was calculated from the formula

$$T_w = T_i - UI\frac{\ln(D_o/D_i)}{2\pi\lambda_t L_t} \,, \tag{2}$$

where T_i was calculated as the arithmetic mean of twelve wall temperatures measured inside:

$$T_w = \frac{\sum\limits_{i=1}^{i=12} T_{wloc}}{12} \,. \tag{3}$$

Wall superheat was estimated as

$$\Delta T = T_w - T_f \,, \tag{4}$$

where T_f was calculated as the arithmetic mean of six measured fluid temperatures (Fig. 1)

$$T_f = \frac{\sum\limits_{i=1}^{i=6} T_{floc}}{6} \,. \tag{5}$$

Mean heat transfer coefficient was calculated as

$$\alpha = \frac{q}{\Delta T} \,. \tag{6}$$

The uncertainties of the measured and calculated parameters are estimated by the mean-square method. The experimental uncertainty of heat flux was estimated as follows:

$$\Delta q = \sqrt{\left(\frac{\partial q}{\partial P}\Delta P\right)^2 \left(\frac{\partial q}{\partial D_o}\Delta D_o\right)^2 + \left(\frac{\partial q}{\partial L}\Delta L\right)^2} \,, \tag{7}$$

where the absolute measurement errors of the electrical power ΔP, outside tube diameter ΔD_o and active length of a tube ΔL are 10 W, 0.02, and 0.2 mm, respectively. So, the maximum overall experimental limits of error for heat flux extended from $\pm 1.3\%$ for maximum heat flux up to $\pm 6.5\%$ for the minimum heat flux. The experimental uncertainty for the average heat transfer coefficient is calculated as

$$\Delta\alpha = \sqrt{\left(\frac{\partial \alpha}{\partial q}\Delta q\right)^2 \left(\frac{\partial \alpha}{\partial \Delta T}\delta T\right)^2} \,, \tag{8}$$

where the absolute measurement error of the wall superheat, δT, estimated from the systematic error analysis equals ± 0.2 K. The maximum error for the average heat transfer coefficient was estimated to be equal to $\pm 9.6\%$.

3 Results

In order to validate the apparatus as well as experimental procedure, the present data were compared to the data reported by other researchers for distilled water boiling on horizontal tubes with porous coatings of about the same thickness ~ 0.15 mm, fabricated by thermal spraying [26–28]. Satisfactory agreement was obtained only with data collected by Cieśliński [26], although different heating methods of the test sections were applied in both cases – Fig. 4. The big discrepancy between the present data and the results obtained by Cieśliński and Krasowski [28] may result from different porosity of the tested porous coatings as well as geometry of the experimental vessel. As an example, Figs. 5 and 6 display boiling curves for water-Al_2O_3 and water-Cu nanofluids, respectively, on smooth tubes at operating pressure of about 100 kPa for three tested nanoparticle concentrations, i.e., 0.01,

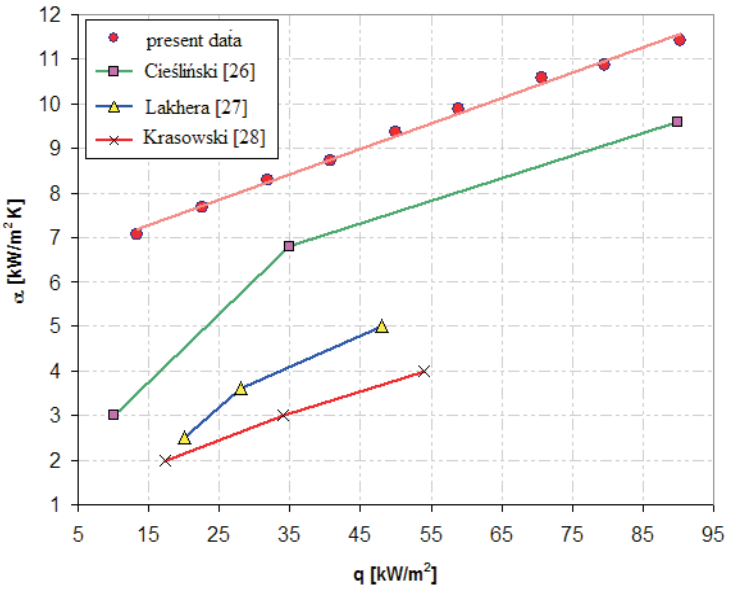

Figure 4: Validation of present experimental results with literature data.

0.1, and 1 wt%. As it is seen in Figs. 5 and 6 addition of nanoparticles results in heat transfer enhancement – the boiling curves are shifted left, towards lower superheats. Moreover, heat transfer enhancement increases with nanoparticle loading increase.

Figure 7 illustrates enhancement factors k_{eff} – defined as a ratio of the heat transfer coefficient for nanofluid to the heat transfer coefficient for distilled water at the same wall superheat (heat flux) for water-Al_2O_3 and water-Cu nanofluids of the same nanoparticle concentration (0.01%), $k_{eff} = \frac{\alpha_{nano}}{\alpha_{water}}$ while boiling on polished ($R_a = 0.06$ μm), and emered ($R_a = 0.11$ μm), stainless steel tube at subatmospheric pressure ($p = 10$ kPa). For both tube surface states enhancement factor decreases with heat flux increase, nevertheless the best fitting line for emered tube is very steep.

Figures 8 and 9 display boiling curves and heat transfer coefficient for water-Al_2O_3 nanofluid on porous coated tube at overpressure for three tested nanoparticle concentrations, i.e., 0.01, 0.1, and 1 wt%. Contrary to smooth and rough tubes boiling curves for water-Al_2O_3 nanofluids are shifted right, towards higher superheats. This means heat transfer deterioration – the greater the higher was a concentration of nanoparticles. Probably, the open pores of the porous coating that served as active nucleation sites during boiling of pure water, were clogged by nanoparticles

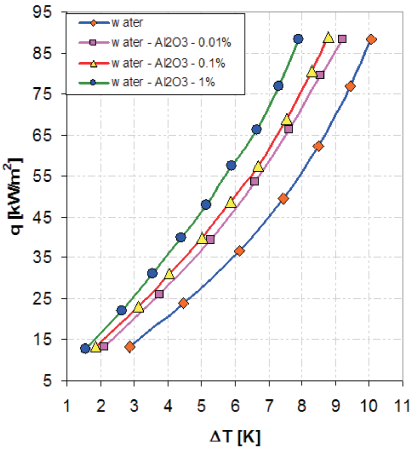

Figure 5: Boiling curves for water-Al_2O_3 nanofluid on polished tube ($R_a = 0.06$ μm) at $p \approx 100$ kPa.

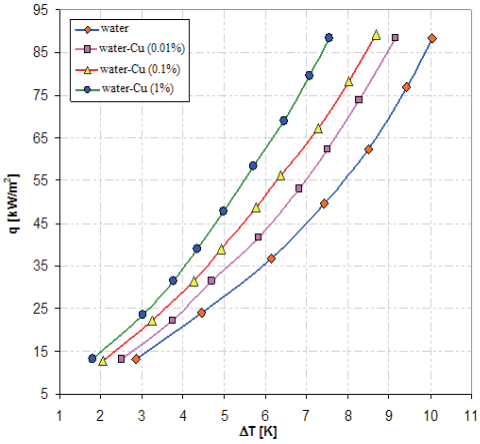

Figure 6: Boiling curves for water-Cu nanofluid on polished tube ($R_a = 0.06$ μm) at $p \approx 100$ kPa.

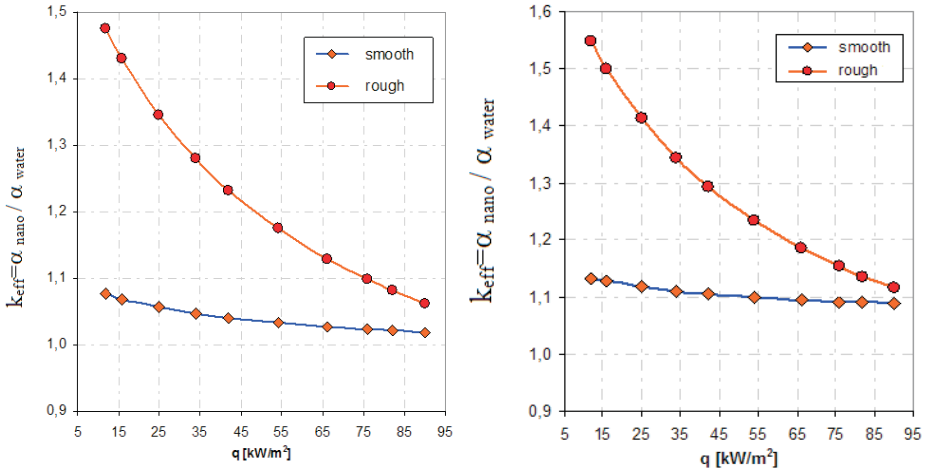

(a) (b)

Figure 7: Enhancement factor for (a) water-Al_2O_3 and (b) water-Cu nanofluids of 0.01% nanoparticle concentration during boiling on rough tubes at $p = 10$ kPa.

during boiling of nanofluids.

The same situation was observed during boiling of water-Cu nanofluids on porous coated tube at overpressure. Independent of tested nanoparticle concentration, i.e., 0.01, 0.1, and 1 wt% , heat transfer inhibition was

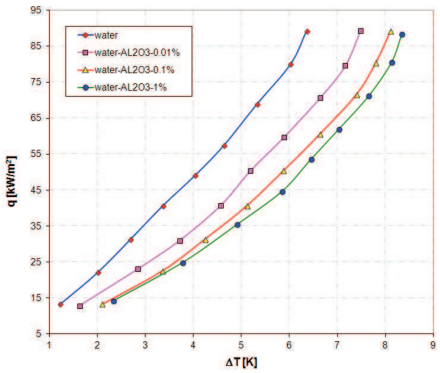

Figure 8: Boiling curves for water-Al_2O_3 nanofluid on porous coated tube at $p = 200$ kPa.

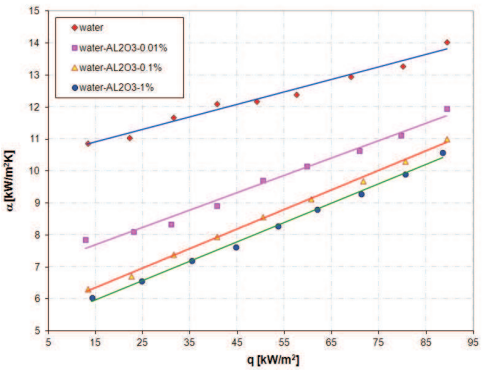

Figure 9: Heat transfer coefficient for water-Al_2O_3 nanofluid on porous coated tube at $p = 200$ kPa.

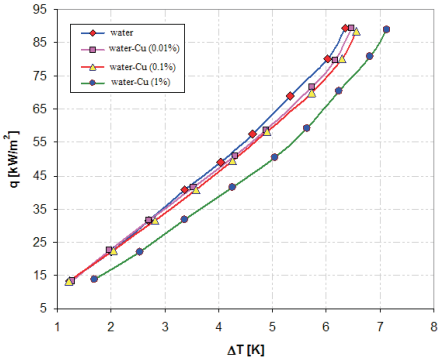

Figure 10: Boiling curves for water-Cu nanofluid on porous coated tube at $p = 200$ kPa.

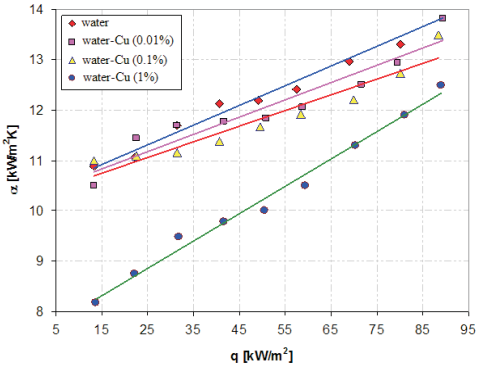

Figure 11: Heat transfer coefficient for water-Cu nanofluid on porous coated tube at $p = 200$ kPa.

recorded. However, as it is seen in Figs. 10 and 11 for nanoparticle concentrations of 0.01 and 0.1% only a slight heat transfer inhibition has been observed, while for 1% nanoparticle concentration dramatic heat transfer deterioration has been recorded, particularly for lower heat fluxes – Fig. 11.

Exemplarily, Figs. 12 and 13 show boiling curves and heat transfer coefficient, respectively, for boiling of water-Cu nanofluid with 0.1% nanoparticle concentration on porous coated tube at different pressures. For both tested nanofluids, i.e., water-Cu and water-Al_2O_3, increase of operating pressure resulted in heat transfer enhancement.

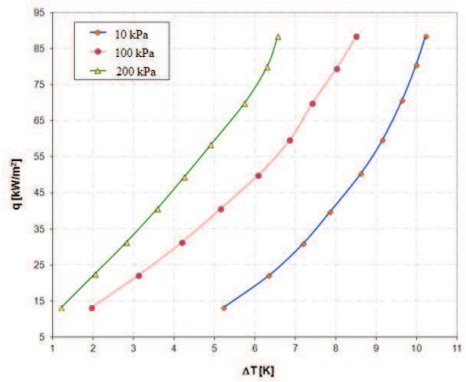

Figure 12: Boiling curves for water-Cu nanofluid with 0.1% nanoparticle concentration on porous coated tube at different operating pressures.

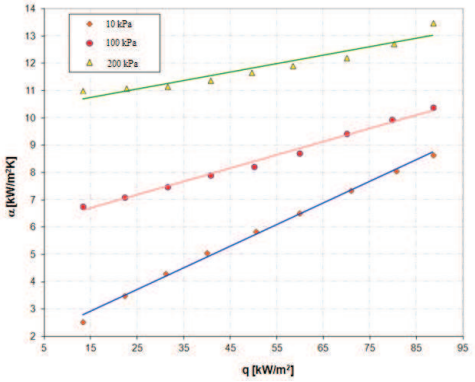

Figure 13: Heat transfer coefficient for water-Cu nanofluid with 0.1% nanoparticle concentration on porous coated tube at different operating pressures.

A multidimensional regression analysis using the least squares method was applied to establish correlation equation for prediction of an average heat transfer coefficient during pool boiling of water-Al_2O_3 and water-Cu nanofluids of different nanoparticle concentration on horizontal rough and porous coated tubes at various operating pressures

$$\mathrm{Nu} = 112\, C_{sf} \mathrm{Bo}^{0.197} \left(\frac{p}{p_{cr}}\right)^{0.0182} \left(\frac{K}{D_p}\right)^{0.03} [(1 - \ln \Phi)^{\Phi}]^{-0.18}\,, \qquad (9)$$

where two key parameters are introduced. First, surface state parameter K, that depends on the the type of a surface and is assumed to be equal to mean surface roughness ($K = R_a$) and mean pore radius ($K = a$) for rough and porous coated surfaces, respectively. Values of the second parameter, (C_{sf}), depend on the liquid-surface combination and are given in Tab. 1.

Table 1: Surface/liquid parameter C_{sf}.

Nanofluid	Surface state	C_{sf}
water-Al_2O_3	rough, stainless steel	1
water-Cu	rough, stainless steel	0.9377
water-Al_2O_3 water-Cu	porous coated	0.759

A comparison of predicted data against the experimentally obtained under the present investigation is displayed in Fig. 14. For about 97% of experimental points the discrepancy between experimental data and values calculated from the proposed correlation is lower than ±25%.

4 Conclusions

Smooth and rough tubes:

- Addition of nanoparticles augments heat transfer during pool boiling of water-Al_2O_3 and water-Cu nanofluids on stainless steel tubes.
- Increase in operating pressure results in heat transfer coefficient enhancement.

Porous coated tubes:

- Independent of operating pressure addition of even small amount of nanoparticles inhibits heat transfer in comparison with boiling of distilled water.
- Heat transfer coefficient decreases with nanoparticle concentration increase.
- Independent of nanoparticle concentration, increase of operating pressure results in heat transfer coefficient increase.

Heat transfer coefficients predicted by use of the proposed Nusselt-type relation correlate satisfactory with the experimental data related to the tested nanofluids over some range of nanoparticle concentration, operating pressure and heat flux below 100 kW/m^2.

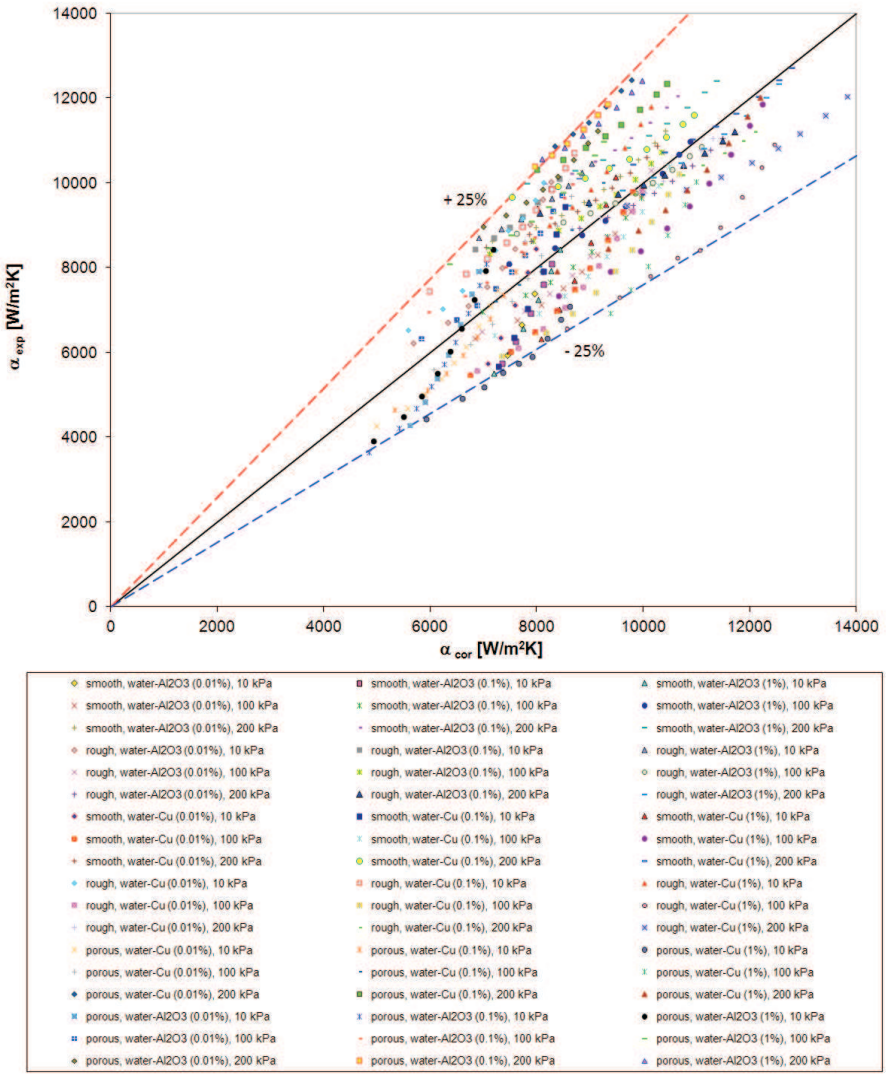

Figure 14: Comparison of the present experimental data with the predictions obtained by use of the proposed correlation Eq. (9).

Acknowledgement This work was sponsored by the Ministry of Research and Higher Education, Grant No. NN512 374435.

Received 12 November 2012

References

[1] Choi S.: *Enhancing thermal conductivity of fluids with nanoparticles*. Developments and Applications of Non-Newtonian Flows, ASME, FED. 231/MD-66(1995) 99–105.

[2] Cieśliński J.T., Kaczmarczyk T.: *Pool boiling of water-Al_2O_3 and water-Cu nanofluids on horizontal smooth tubes*. Nanosc. Res. Lett. (2011), 6–220, doi:10.1186/1556-276X.

[3] Barber J., Brutin D., Tadrist L.: *A review on boiling heat transfer enhancement with nanofluids*. Nanosc. Res. Lett. (2011), 6:280.

[4] Cieśliński J.T.: *Improved heat transfer to water boiling on tubes covered with porous metallic coatings*. Arch. Thermodyn. **16**(1995), 1-2, 93–101.

[5] Cieśliński J.T.: *Nucleate pool boiling heat transfer of water from gas-thermally coated surfaces*. Arch. Thermodyn. **13**(1992), 1–4, 49–57.

[6] Cieśliński J.T.: *An experimental study of nucleate pool boiling heat transfer from a flat horizontal plate covered with porous coatings*. Arch. Thermodyn. **12**(1991), 1–4, 69–76.

[7] Wang X.Q., Mujumdar A.S.: *Heat transfer enhancement of nanofluids: A review*. Int. J. Thermal Sci. **46**(2007), 1–9.

[8] Godson L., Raja B., Lal D.M., Wongwises S.: *Enhancement of heat transfer using nanofluids – An overview*. Renew. Sust. Energ. Rev. **14**(2010), 629–641.

[9] Das S.K., Putra N., Roetzel W.: *Pool boiling characteristics of nano-fluids*. Int. J. Heat Mass Transf. **47**(2003), 851–862.

[10] Das S.K., Putra N., Roetzel W.: *Pool boiling of nano-fluids on horizontal narrow tubes*. Int. J. Multiphase Flow **29**(2003), 1237–1247.

[11] Khandekar S., Joshi Y.M., Mehta B.: *Thermal performance of closed two-phase thermosyphon using nanofluids*. Int. J. Thermal Sci. **47**(2008), 659–667.

[12] Chopkar M., Das A.K., Manna I., Das P.K.: *Pool boiling heat transfer characteristics of ZrO_2-water nanofluids from a flat surface in a pool*. Heat Mass Transf. **44**(2008), 999–1004.

[13] Suriyawong A., Wongwises S.: *Nucleate pool boiling heat transfer characteristics of TiO_2-water nanofluids at very low concentrations*. Exp. Thermal Fluid Sci. **34**(2010), 992–999.

[14] Narayan G. P., Anoop K. B., Das S. K.: *Mechanism of enhancement/ deterioration of boiling heat transfer using stable nanoparticle suspensions over vertical tubes*. J. Appl. Phys. **102**(2007), 074317.

[15] Liu Z., Xiong J., Bao R.: *Boiling heat transfer characteristics of nanofluids in a flat heat pipe evaporator with micro-grooved heating surface*. Int. J. Multiphase Flow **33**(2007), 1284–1295.

[16] Yang Ch., Liu Da.: *Pool boiling on plain and enhanced tubes of refrigerant R141b with nanoparticles*. Proc. 5th Int Conf. on Multiphase Flow, ICMF-2004, Yokohama, No. 365.

[17] Das S.K., Putra N., Roetzel W.: *Pool boiling characteristics of nano-fluids*. Int. J. Heat Mass Transf. **47**(2003), 851–862.

[18] Cornwell K., Houston S.D: *Nucleate pool boiling on horizontal tubes: a convection-based correlation*. Int. J. Heat Mass Transf. **37**(1994), 303–309.

[19] Shi M. H., Shuai M. Q., Lai Y. E., Li Y. Q., Xuan M.: *Experimental study of pool boiling heat transfer for nanoparticle suspensions on a plate surface*. Proc. 13th Int. Heat Transfer Conf., Sydney, 2006, BOI-06 (CD-ROM).

[20] Rohsenow W.M.: *A method of correlating heat transfer data for surface boiling liquids*. ASME C **74**(1952), 969–976.

[21] Das S., Bhaumik S.: *A correlation for the prediction of heat flux for nucleate pool boiling heat transfer of nanofluid*. Arab. J. Sci. Eng. doi: 10.1007/s13369-014-1081-z.

[22] Stephan K., Abdelsalam M.: *Heat transfer correlations for natural convection boiling*. Int. J. Heat Mass Transf. **23**(1980), 73–87.

[23] Peng H., Ding G., Hu H.: *Effect of surfactant additives on nucleate pool boiling heat transfer of refrigerant-based nanofluid*. Experimental Therm. Fluid Sci. **35**(2011), 960–970.

[24] Pal P., Bhaumik S.: *Development of Theoretical Correlation for Prediction of Boiling Heat Transfer Using water-TiO2 Nanofluid*. Proc. 2012 Int. Conf. on Environment, Energy and Biotechnology, IPCBEE **33**(2012), IACSIT Press, Singapore.

[25] Suriyawong A., Dalkilic A.S., Wongwises S.: *Nucleate Pool Boiling Heat Transfer Correlation for TiO_2-Water Nanofluids*. J. ASTM Int. **9**(2012), 5, ID JAI104409.

[26] Cieśliński J.T.: *Nucleate pool boiling on porous metallic coatings*. Exp. Therm. Fluid Sci. **25**(2002), 557–564.

[27] Lakhera V.J., Gupta A., Kumar R.: *Investigation of coated tubes in cross-flow boiling*. Int. J. Heat Mass Transf. **52**(2009), 908–920.

[28] Cieśliński J.T., Krasowski K.: *Heat transfer during pool boiling of water, methanol and R141b on porous coated horizontal tube bundles*. J. Enhanc. Heat Transf. **20**(2013), 2, 165–177.